

Reaction Development and Mechanistic Study of a Ruthenium Catalyzed Intramolecular Asymmetric Reductive Amination en Route to the Dual Orexin Inhibitor Suvorexant (MK-4305)

Neil A. Strotman,^{*,†} Carl A. Baxter,[‡] Karel M. J. Brands,[†] Ed Cleator,[‡] Shane W. Krska,[†] Robert A. Reamer,[†] Debra J. Wallace,[†] and Timothy J. Wright[§]

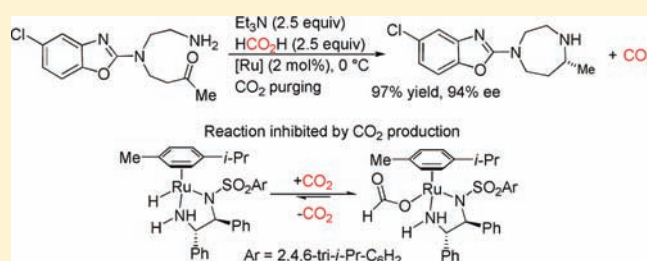
[†]Department of Process Chemistry, Merck Research Laboratories, Rahway, New Jersey 07065, United States

[‡]Department of Process Chemistry, Merck Sharp and Dohme Research Laboratories, Hertford Road, Hoddesdon, Hertfordshire, EN11 9BU, U.K.

[§]Department of Chemical Engineering, Merck and Company, Rahway, New Jersey 07065, United States

S Supporting Information

ABSTRACT: The first example of an intramolecular asymmetric reductive amination of a dialkyl ketone with an aliphatic amine has been developed for the synthesis of Suvorexant (MK-4305), a potent dual Orexin antagonist under development for the treatment of sleep disorders. This challenging transformation is mediated by a novel Ru-based transfer hydrogenation catalyst that provides the desired diazepane ring in 97% yield and 94.5% ee. Mechanistic studies have revealed that CO₂, produced as a necessary byproduct of this transfer hydrogenation reaction, has pronounced effects on the efficiency of the Ru catalyst, the form of the amine product, and the kinetics of the transformation. A simple kinetic model explains how product inhibition by CO₂ leads to overall first-order kinetics, but yields an apparent zero-order dependence on initial substrate concentration. The deleterious effects of CO₂ on reaction rates and product isolation can be overcome by purging CO₂ from the system. Moreover, the rate of ketone hydrogenation can be greatly accelerated by purging of CO₂ or trapping with nucleophilic secondary amines.



INTRODUCTION

Merck & Co. recently disclosed the evaluation of the novel dual Orexin antagonist **1** (Suvorexant, MK-4305) as a potential treatment for insomnia in phase III clinical trials (Figure 1).¹ The first multikilogram synthesis of **1** was recently reported.² However, preparation of the chiral diazepane ring moiety was achieved through a racemic reductive amination and classical resolution sequence to afford a 27% overall yield from 2-MSA to (*R*)-**3** (Scheme 1). It was projected that performing the reductive amination in an asymmetric fashion would remove a step from the synthesis and greatly improve the overall yield and productivity of the synthesis.

The racemic process alone faces a series of challenges: the requirement for preferential reduction of imine over acyclic ketone, a challenging 7-membered ring formation, and the need for intra- versus intermolecular reaction. In addition to these concerns, an asymmetric process presents the added difficulty of providing chiral induction at an imine showing little steric differentiation (Me vs CH₂CH₂NR₂) (Scheme 2).³ Despite these challenges, we report the first asymmetric reductive amination of a dialkyl ketone with an alkyl amine. In addition, mechanistic studies have provided insight toward the structures

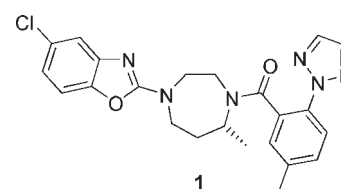


Figure 1. Dual Orexin antagonist MK-4305 (**1**).

of the species involved in the catalytic cycle and uncovered the profound effect of CO₂ on the equilibrium levels of the active catalyst and rate of reaction.

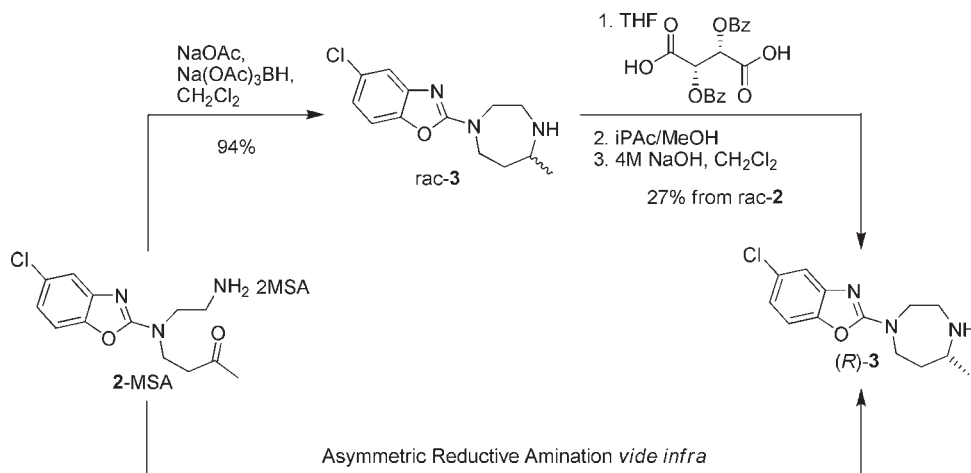
DEVELOPMENT OF ASYMMETRIC REDUCTIVE AMINATION

A variety of different approaches were considered for the transformation of 2-MSA (MSA: methanesulfonic acid) to (*R*)-**3** (via **4**) including direct hydrogenation (H₂) and transfer

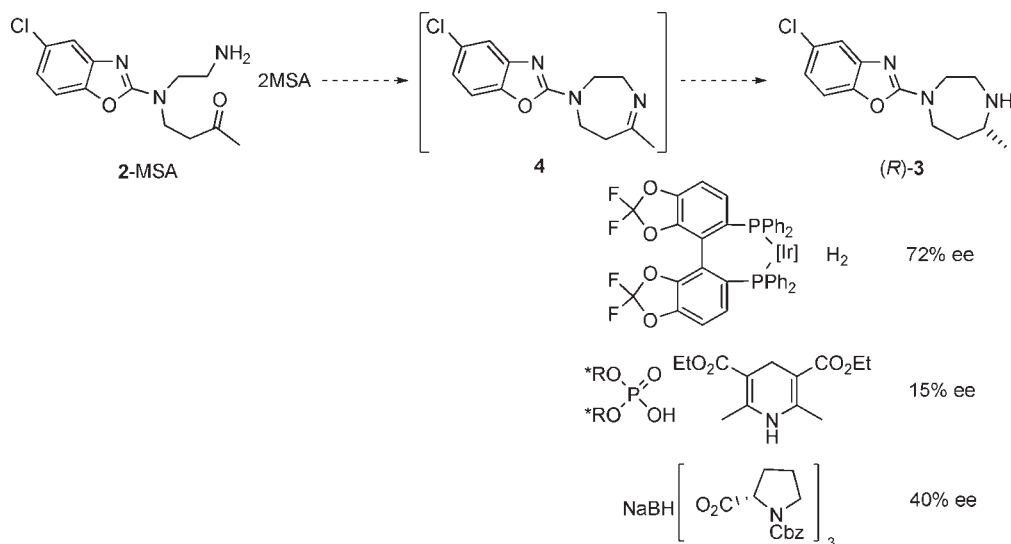
Received: March 15, 2011

Published: May 02, 2011

Scheme 1. Racemic and Asymmetric Reductive Amination Routes



Scheme 2. Asymmetric Reductive Amination of 2-MSA



hydrogenation (HCO_2H or 2-propanol (IPA)), which are both known to give faster reduction of imines than ketones (Scheme 2).⁴ An extensive screen of direct hydrogenation conditions involving Rh, Ir, Ru, and Pd precatalysts with ~ 200 chiral phosphine ligands resulted in up to 72% ee for (*R*)-3 (Scheme 2).^{5,6} Other approaches involving a chiral phosphoric acid catalyst³ or a chiral borohydride⁷ provided the product in significantly lower enantioselectivities (15 and 40% ee, respectively; Scheme 2).

Given these moderate enantioselectivities, we turned our attention to transfer hydrogenation conditions⁸ using variants of Noyori's (*S,S*)-RuCl(*p*-cymene)(TsDPEN) (**5**) (TsDPEN = *N*-tosyl-1,2-diphenylethylenediamine) catalyst, which have proven useful for reduction of both ketones⁹ and imines.⁴ While there are a few successful examples of the use of this catalyst for asymmetric reductive amination of alkyl-aryl ketones (acetophenones),¹⁰ only very poor selectivities have been achieved for dialkyl ketones or even alkyl-aryl ketones in an intramolecular sense.^{11,12} Studies on transfer hydrogenation of ketones to produce alcohols involving modifications to this TsDPEN ligand suggested that the reactivity and

enantioselectivity could be highly influenced through changes to the ligand architecture.¹³ An evaluation of 30 ligand analogues based on both DPEN and *trans*-1,2-diaminocyclohexane (DACH) scaffolds (Figure 2) showed some promising product enantioselectivities (Table 1, entries 1–7). Although the parent TsDPEN ligand gave essentially racemic product (entry 1), the product enantioselectivity was improved significantly by using more sterically bulky ligands (entries 3 and 4), with the 2,4,6-triisopropylphenylsulfonyl-DPEN ligand (TIPPS-DPEN, **9**) proving to be the most effective. A notably higher ee was obtained in MeCN than in IPA, THF, 5:2 formic acid/ Et_3N , or in a variety of other solvents.

Both the enantioselectivity and yield were improved dramatically when no effort was made to preform imine **4** (entry 8).¹⁴ Changing the η^6 arene portion of the catalyst to benzene or hexamethylbenzene led to decreased selectivity (entries 9 and 10). Moving to the isoelectronic pentamethylcyclopentadienyl (Cp^*) rhodium or iridium analogues (entries 11 and 12) failed to produce any improvement.¹⁵ Reducing the temperature from 35 to 0 °C for the reaction in MeCN not only afforded the expected increase in enantioselectivity, but also led to a large increase in yield

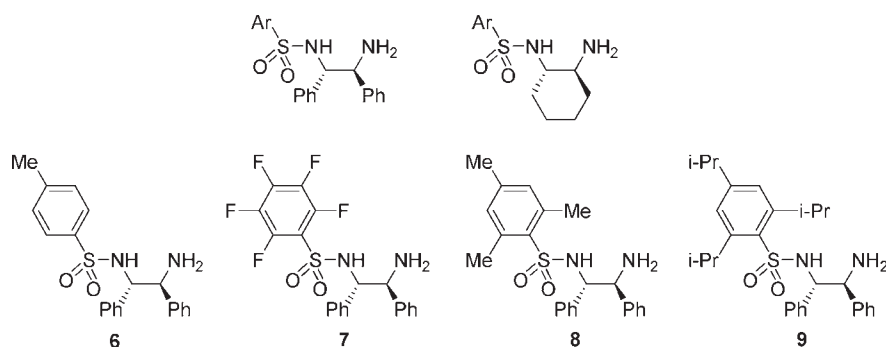
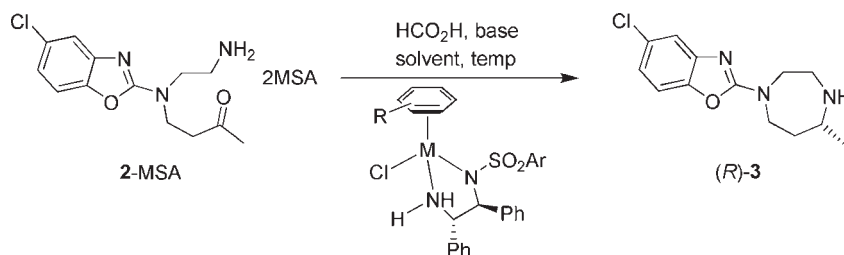


Figure 2. Select transfer hydrogenation ligands employed in this study.

Table 1. Optimization of Asymmetric Reductive Amination Using Transfer Hydrogenation Catalysts



entry	ligand	M	arene	solvent	temp (°C)	HCO ₂ H (equiv)	Et ₃ N (equiv)	other base (equiv)	ee (%)	assay yield (%)
1 ^a	6	Ru	<i>p</i> -cymene	MeCN	35	5	2	NaO ₂ CH	19	45
2 ^a	7	Ru	<i>p</i> -cymene	MeCN	35	5	2	NaO ₂ CH	13	31
3 ^a	8	Ru	<i>p</i> -cymene	MeCN	35	5	2	NaO ₂ CH	46	21
4 ^a	9	Ru	<i>p</i> -cymene	MeCN	35	5	2	NaO ₂ CH	52	19
5 ^a	9	Ru	<i>p</i> -cymene	THF	35	5	2	NaO ₂ CH	39	31
6 ^a	9	Ru	<i>p</i> -cymene	IPA	35	5	2	NaO ₂ CH	42	28
7 ^a	9	Ru	<i>p</i> -cymene	none	35	100	40	NaO ₂ CH	21	39
8	9	Ru	<i>p</i> -cymene	MeCN	35	5	4		70	54
9	9	Ru	benzene	MeCN	35	5	4		30	33
10	9	Ru	Me ₆ C ₆	MeCN	35	5	4		9	42
11	9	Rh	Cp*	MeCN	35	5	4		45	11
12	9	Ir	Cp*	MeCN	35	5	4		37	38
13	9	Ru	<i>p</i> -cymene	DCM	35	5	4		71	53
14	9	Ru	<i>p</i> -cymene	MeCN	0	5	4		80	72
15	9	Ru	<i>p</i> -cymene	DCM	0	5	4		80	59
16	9	Ru	<i>p</i> -cymene	MeCN	0	5	0	K ₂ CO ₃ (4)	84	82 ^b
17	9	Ru	<i>p</i> -cymene	MeCN	0	5	0	K ₃ PO ₄ (4)	86	54 ^c
18	9	Ru	<i>p</i> -cymene	MeCN	0	3.5	2.5	K ₂ CO ₃ (4)	90	88
19 ^d	9	Ru	<i>p</i> -cymene	DCM	-5	2.5	2.5	K ₂ CO ₃ (4)	94	>96
20 ^d	9	Ru	<i>p</i> -cymene	MeCN/PhMe	0	2.5	2.5	K ₂ CO ₃ (4)	94.5	>97

^a Aged substrate at 40 °C with NaO₂CH (2 equiv) and MgSO₄ for 2 h prior to start of reaction to form the imine. ^b 82% yield at 93% conversion. ^c 54% yield at 72% conversion. ^d Combined substrate with 4 equiv K₂CO₃ in solvent and 0.1 vol of water to carry out deprotonation, and filtered before use.

(entry 14 vs 8). Although a similar increase in enantioselectivity was observed in CH₂Cl₂ upon lowering the temperature, the yield increase was minimal (entries 13 and 15). When examining the effect of other bases on this process, it was discovered that while inorganic bases led to slower reaction rates, employing K₂CO₃ or K₃PO₄ did lead to an increase in ee (entries 16 and 17).

Further optimization of this system revealed that a mixture of K₂CO₃ and Et₃N provided both high product selectivities and high reaction rates. By simultaneously optimizing the concentrations of substrate, HCO₂H, Et₃N, and K₂CO₃, 90% ee and 88% yield was

achieved for this process using only 3 mol % catalyst (entry 18). It was eventually found that the beneficial role of inorganic base was to precipitate the mesylate counterion as KOMs.¹⁶ By first deprotonating 2-MSA with K₂CO₃ and then filtering, this reaction performed exceptionally well in DCM, providing the product in 94% ee and nearly quantitative yield (entry 19). When these asymmetric reductive amination conditions were implemented on a larger scale, 3 was formed in 94% ee and >97% yield (Scheme 3). The amine could be isolated in a single operation as its HCl salt 3-HCl in 87% overall yield and affording >99.5% ee.¹⁷ Alternatively, CH₂Cl₂ could

Scheme 3. Asymmetric Reductive Amination

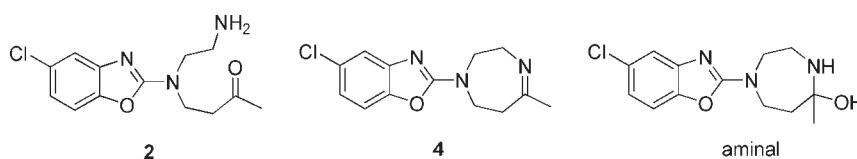
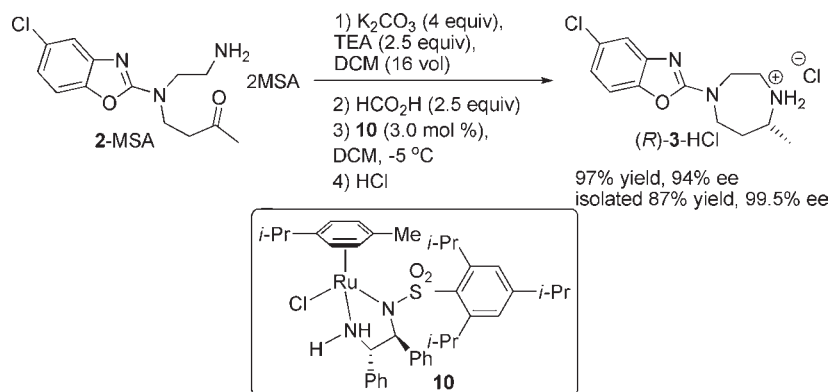
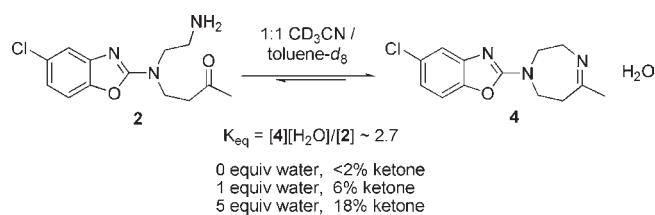


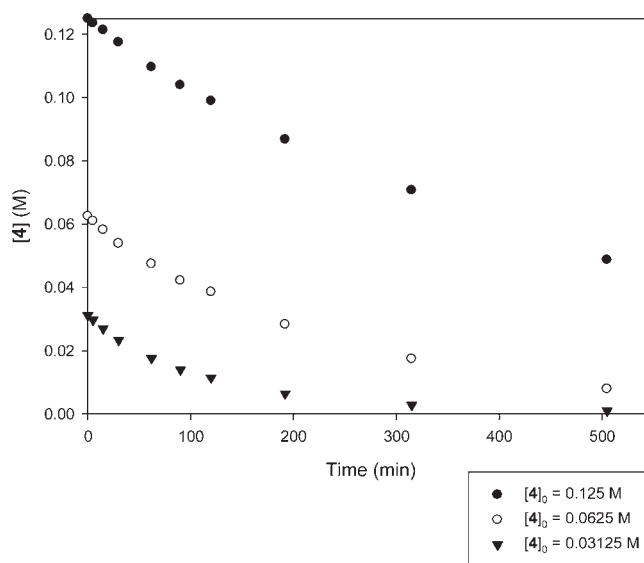
Figure 3. Possible forms of the free-base of 2-MSA.

Scheme 4. Equilibrium between Ketone and Imines form of **2** Free Base

be replaced with a 1:1 mixture of MeCN/toluene, giving the same high selectivity and yield (entry 20).¹⁸ The level of enantioselectivity obtained in this reaction is remarkable considering that this is the only example of asymmetric reductive amination of a dialkylketone with an aliphatic amine.

At this point, the asymmetric reductive amination reaction was examined in more detail to determine if any further improvements in productivity (higher rate, lower catalyst loading, lower solvent volume, etc.) could be made. Until now, the form in which the free-base of 2-MSA existed had not been studied and the relative contributions of ketone, imine, and aminal were not known (Figure 3). While RPLC-MS showed exclusively the mass of the ring-opened ketone form (**2**) (or aminal), it was hypothesized that imine **4**, which should be the actual species undergoing transfer hydrogenation, was likely the major species under the nearly anhydrous reaction conditions. More importantly, if the imine were not the major form, the transfer hydrogenation could be greatly accelerated if conditions were altered to favor formation of this species.

1H NMR spectroscopy in CD_2Cl_2 showed the presence of primarily **4**, with only 5–10% of **2** and no signals for the corresponding aminal. Although the NMR signals for compounds **4** and **2** showed similar coupling patterns, ^{13}C NMR spectroscopy clearly showed the ketone carbonyl in the minor species (**2**) (δ 207.3 ppm).

Figure 4. $[4]$ vs time at various initial concentrations of **4**.

Since even 1 equiv of water proved immiscible in CD_2Cl_2 , the equilibrium was studied in a 1:1 mixture of CD_3CN /toluene- d_8 . The equilibrium lies almost completely toward the imine isomer when no water is added (Scheme 4). Even with the addition of 5 equiv of water, the equilibrium still greatly favors the imine isomer with a K_{eq} of 2.7. It is interesting to note that, as in CD_2Cl_2 , the corresponding aminal species was not observed. Addition of triethylamine or formic acid did not affect the position of the equilibrium.

KINETICS OF REDUCTIVE AMINATION

The kinetic behavior of the reaction network was studied as part of an effort to reduce the catalyst loading for the asymmetric

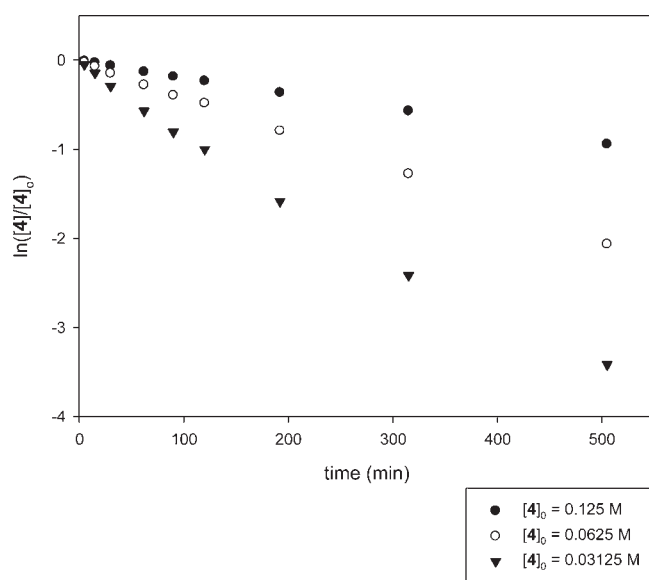


Figure 5. $\ln([4]_t/[4]_0)$ vs time at various initial concentrations of 4.

Table 2. Observed Rate Constants (k_{obs}) and Initial Rates As a Function of Initial Substrate Concentration at 0 °C

$[4]_0$ (M)	$k_{\text{obs}} = (-d[4]/dt)/[4]_0$ (s^{-1})	initial rate = $k_{\text{obs}}[4]_0$ (M s^{-1})
0.1250	$3.56 \pm 0.26 \times 10^{-5}$	4.45×10^{-6}
0.0625	$7.31 \pm 0.31 \times 10^{-5}$	4.57×10^{-6}
0.03125	$15.6 \pm 0.43 \times 10^{-5}$	4.88×10^{-6}

reductive amination step. An initial experiment under the standard conditions (0.125 M of 4 in 1:1 MeCN/toluene) provided a curve that appeared to be overall first-order (Figure 4) and yielded a linear plot of $\ln[4]$ versus time (Figure 5).^{19–21} Surprisingly, when the same experiment was performed with $[4]_0$ at 0.0625 M, the observed rate constant ($k_{\text{obs}} = (-d[4]/dt)/[4]$), was twice that seen at the higher concentration rather than being identical, as expected (Table 2). When the concentration of 4 was decreased further to 0.03125 M, the k_{obs} again doubled, indicative of a zero-order dependence on 4. This raised the question of how a reaction that has no apparent order in substrate (rate is independent of $[4]_0$) could at the same time appear to follow overall first-order kinetics.

Elegant kinetic experiments performed by Wills and co-workers using tethered derivatives of 5 have demonstrated that transfer hydrogenation may initially be zero-order in substrate, when substrate concentration is high and catalyst regeneration is rate-limiting, but become first-order in substrate as the reaction progresses and substrate reduction becomes rate-limiting.²² Depending on the exact catalyst derivative that Wills employed, kinetics varied widely between exhibiting complete first-order behavior and nearly complete zero-order behavior. Our kinetic curves are dominated by first-order kinetics, presumably due to a first-order dependence on [4], which is emphasized in the log plots. However, a first-order dependence on [4] should render log plots with the same slope regardless of the initial concentration of 4, contrary to what we observed.

The observed reaction kinetics are strongly suggestive of product inhibition, where the reaction rate decreases as the product concentration increases. However, it was difficult to

imagine how 3 could inhibit this reaction since other secondary amines had proven essentially inert. Another possibility was reversibility of the transfer hydrogenation reaction. The fact that the enantioselectivity of 3 did not erode upon extended reaction times, and that subjecting enantiopure (*R*)-3 to the reaction conditions did not produce any of the undesired enantiomer ((*S*)-3) did not support this. Another possibility was a dependence of the rate on the concentration of formic acid, but a series of experiments showed that this was not the case. The only remaining hypothesis was that the CO_2 being produced throughout the reaction was causing the inhibition, although it is generally believed that CO_2 extrusion by transfer hydrogenation catalysts is irreversible.^{9b} To test this hypothesis, the transfer hydrogenation reaction was conducted under standard conditions with addition of CO_2 : a >10-fold decrease in rate was observed. This observation of CO_2 inhibition prompted us to fully explore the origin of this previously unreported phenomenon.

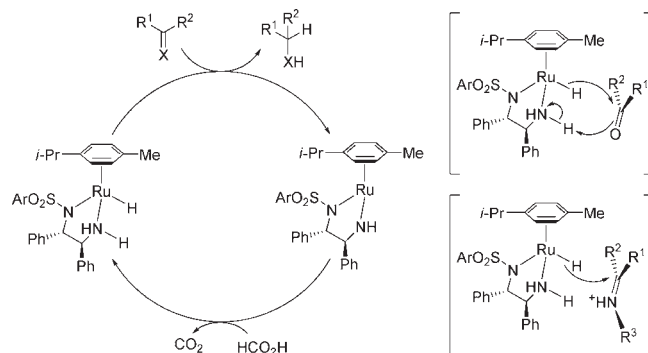
STUDY OF CATALYTIC SPECIES

Transfer hydrogenation using Noyori's $\text{RuCl}(\textit{p}\text{-cymene})$ - (TsDPEN) catalyst is believed to proceed through a pathway wherein an 18-electron Ru–hydride undergoes either concerted proton and hydride addition to a ketone²³ or hydride transfer to an imine or iminium species^{24,25} to produce an alcohol or amine, respectively, and generate an unsaturated 16-electron Ru species (Scheme 5).^{4,9,22} With formic acid as the terminal hydrogen donor, the Ru–hydride is regenerated, producing CO_2 as a byproduct.

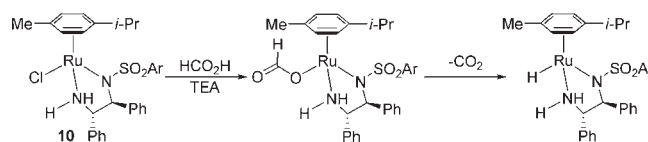
A study was undertaken to investigate by ^1H NMR spectroscopy how rapidly the precursor 10 reacts with triethylamine and formic acid to irreversibly generate the active Ru–hydride catalyst. Within 2 min at -5 °C, precursor 10 was completely consumed, indicating very rapid activation. However, two surprising observations emerged from this study.

First, despite the disappearance of 10, Ru–hydride was not the only, or even the major species formed (Scheme 6). It was

Scheme 5. Mechanism of Transfer Hydrogenation Using $\text{RuCl}(\textit{p}\text{-cymene})$ (ArSO_2DPEN) Catalysts



Scheme 6. Conversion of Ru–Chloride to Ru–Hydride via Ru–Formate



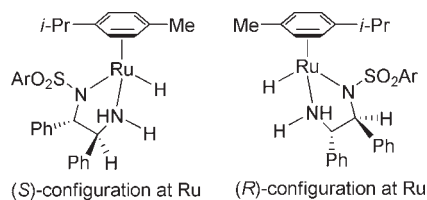


Figure 6. Diastereomers of RuH(*p*-cymene)(ArSO₂-DPEN).

shown that a 95:5 mixture of a species identified as the Ru–formate complex and the anticipated Ru–hydride complex was formed. The assignment of the Ru–formate species was made based on the integration of a high frequency formate proton (separated from a resonance for HCO₂[−] HNEt₃⁺) and the TIPPS-DPEN and *p*-cymene ligands. A thorough search of the literature revealed that this type of species had only been reported once before by Ikariya, who had monitored the rate of decomposition of Ru–formate(*p*-cymene)(TsDPEN) to Ru–hydride.²⁶ Longer age times (>3 h) of the mixture at −5 °C did not lead to additional conversion from the Ru–formate to the Ru–hydride species. This was surprising since conversion of Ru–formate to Ru–hydride is a necessary step in the transfer hydrogenation of **4**, but was occurring at a significantly slower rate than the catalytic reaction proceeds. The only explanation that we could see for this behavior was the existence of an equilibrium between the Ru–formate and Ru–hydride species, which will be discussed below.²⁷

The second surprising observation was that the RuH(*p*-cymene)(TIPPS-DPEN) was not a single species as anticipated, but instead existed as a 3:1 ratio of two species showing hydride resonances at −5.63 and −5.62 ppm, respectively. After 30 min at −5 °C, this ratio had completely switched to 1:2, where it remained. These signals result from the two diastereomers of the catalyst, due to chirality at Ru (Figure 6). A NOESY experiment showed an NOE from the Ru–H at −5.63 ppm to the CHNH₂ methine proton, which can only be achieved in the isomer bearing an (*S*)-configuration at Ru. Likewise, an NOE was seen from the Ru–H at −5.62 to the CHNSO₂ methine proton, consistent with a structure having an (*R*)-configuration at Ru. Noyori reported, based on X-ray crystallographic analysis, that the major diastereomer in RuH(*p*-cymene)(TsDPEN) contains the (*R*)-configuration at Ru (<1% minor diastereomer by NMR spectroscopy).²⁸ More recently Wills demonstrated that tethered variants of **5** can exist as mixtures of diastereomers and that this ratio of diastereomers may change over the course of a reaction.²⁹

Preparation of RuH(*p*-cymene)(TsDPEN) by treatment of RuCl(*p*-cymene)(TsDPEN) with formic acid and triethylamine was also examined by ¹H NMR spectroscopy. Initially, a 65:1 isomer ratio was observed, consistent with Noyori's observations. As expected, the major isomer (Ru–hydride resonance at −5.83 ppm) showed an NOE from the hydride proton to the CHNSO₂ proton, consistent with the (*R*)-configuration at Ru. Interestingly, after 2 h at room temperature, the ratio had changed to ~8:1 due a growth of the resonance corresponding to the minor isomer at −6.13 ppm. This isomerization between the two diastereomers may occur through the 16-electron unsaturated intermediate, which is generated after each hydride transfer event, and which can add hydrogen from formic acid to either catalyst face generating both diastereomers. Diastereomer inter-conversion could also be achieved through partial dissociation of the ArSO₂-DPEN ligand and coordination to the opposite face of

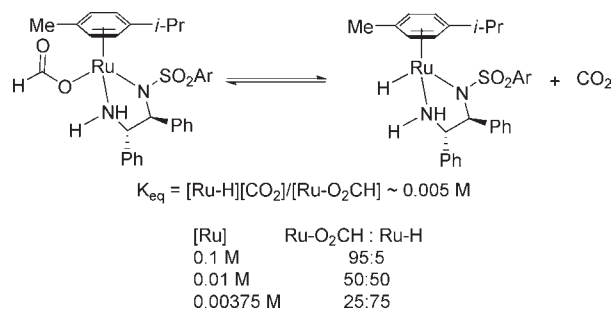


Figure 7. Equilibrium between Ru–formate and Ru–hydride.

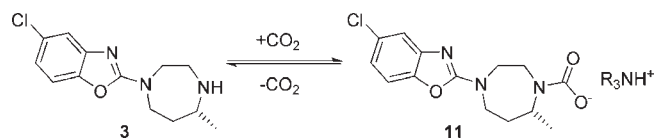
Ru. While both the TIPPS and Ts substituted Ru–hydrides favor the (*R*)-configuration at Ru, it is interesting that such a high level of the (*S*)-isomer is present, especially with the TIPPS substituent. Since the rate of isomerization of RuH(*p*-cymene)(TIPPS-DPEN) is so high even at −5 °C, we were unable to determine if both diastereomers are competent catalysts for transfer hydrogenation, or if both give similar product enantioselectivities or reaction rates.

The potential equilibrium between Ru–formate and Ru–hydride species was studied with the RuH(*p*-cymene)(TsDPEN) catalysts rather than the TIPPS analogue because it provided NMR spectra that were much clearer and easier to interpret. RuH(*p*-cymene)(TsDPEN) was generated from the Ru–chloride complex using Noyori's method with KOH in IPA^{10a} and a solution of the resulting Ru–hydride in CD₂Cl₂ was exposed to CO₂. Resonances were immediately seen for a Ru–formate complex, including a diagnostic high frequency resonance for O₂CH, and complete disappearance of the Ru–hydride resonances. This result provided definitive evidence for the reversibility of Ru–formate conversion to Ru–hydride since CO₂ was the only possible source of formate.³⁰

Similar to experiments with RuCl(*p*-cymene)(TIPPS-DPEN), a 0.1 M solution of RuCl(*p*-cymene)(TsDPEN) was treated with formic acid and triethylamine, and a ~95:5 mixture of Ru–formate to Ru–hydride was observed. However, as the concentration of the Ru–chloride solution was lowered to concentrations which are more similar to those used in the actual asymmetric reductive amination reaction (0.00375 M; equivalent to [Ru] at 3 mol % catalyst), the proportion of Ru–hydride increased greatly (Figure 7). This shift toward the right in the equilibrium can be explained by a concomitant decrease in [CO₂] as the total concentration of Ru is decreased. These equilibrium ratios provide a rough estimate of the equilibrium constant of ~0.005 M, although there is significant error in this estimate since the CO₂ that is generated partitions between the solvent and the headspace of the NMR tube. When the 75:25 mixture of Ru–hydride/Ru–formate was treated with CO₂, all NMR resonances associated with the Ru–hydride disappeared to give the Ru–formate complex as the only Ru species,³¹ providing further evidence for an equilibrium process.

These dramatic effects of CO₂ on the proportion of Ru–hydride present in the reaction mixture help to explain the kinetic observations involving CO₂ inhibition. However, the possibility that CO₂ could interact with the substrate by forming a carbamate with **2**, lowering the concentration of **4** and hence leading to a slower reaction rate, was also considered. No more than a trace of this carbamate species (<2%) was observed when a solution of **2/4** in CD₂Cl₂ was charged with CO₂. The product of the transfer

Scheme 7. Equilibrium between 3 and 11



hydrogenation (3), on the other hand, readily formed carbamate 11 when CO₂ was added, with the ratio of 11:3 increasing with higher CO₂ pressure and lower temperature (Scheme 7). An HMBC experiment conducted on 11 demonstrated a correlation between the carbamate carbon (δ 160.9 ppm) and the three protons geminal to the carbamate nitrogen, providing strong evidence for this structural assignment, and differentiating it from a protonated form of 3.

FURTHER KINETIC STUDIES

The kinetics of the transfer hydrogenation reaction were further investigated by NMR spectroscopy. When the transfer hydrogenation reaction was carried out at 0 °C, 3, 4, 11, and the Ru-hydride could be monitored (Figure 8).³² The [Ru-hydride] reached a maximum at ~1 h, and then slowly decreased to ~40% of this maximum value over the course of the reaction. Throughout the reaction, both the [3] and the [11] increased, maintaining a ratio of ~1.2:1 favoring carbamate 11. It is interesting to note that the reaction of 3 with CO₂ to form 11 reduces the amount of CO₂ in the system, attenuating the deleterious effect of CO₂ on the transfer hydrogenation reaction. Disappearance of 4 followed approximate first-order kinetics with $k_{\text{obs}} = 8.81 \pm 0.16 \times 10^{-5} \text{ s}^{-1}$, showing a 2.5-fold increase from earlier experiments run at -5 °C.³³

Starting from the differential rate expression (eq 1) derived from the catalytic cycle (Scheme 8), and employing a steady-state approximation for the Ru-hydride species (eq 2), eq 3 can be derived. Since [Ru-hydride] had been measured throughout the reaction, eq 1 could be solved for k_2 . A value of $k_2 = 0.22 \pm 0.02 \text{ M}^{-1} \text{ s}^{-1}$ was obtained.³⁴ Rate constant k_1 can be obtained from eq 3, which, at high [4] (early in the reaction), may be simplified to $-d[4]/dt = k_1[Ru]_0$, giving $k_1 = 0.0025 \text{ s}^{-1}$. Finally, $k_{-1} = 0.18 \text{ M}^{-1} \text{ s}^{-1}$ was obtained from the equilibrium expression $K_{\text{eq}} = k_1/k_{-1}$ which relates Ru-hydride and CO₂ with Ru-formate.³⁵

However, eq 3 still contains [CO₂], and therefore, an analytical solution expressed only in terms of [4] cannot be offered. An accurate representation of [CO₂] in terms of [4] must include its generation as the reaction progresses, the equilibrium with amine 3 to give carbamate 14, and partitioning between the solution and gas phases in the reaction vessel.³⁶ However, a simple approximation is $[CO_2] = [4]_0 - [4]$, where an equimolar amount of CO₂ is generated as imine 4 is consumed. Substituting this expression into eq 3 yields eq 4. Since the term $k_{-1}[4]_0$ is much larger than $(k_2 - k_{-1})[4] + k_1$ (due to similar values of rate constants k_2 and k_{-1} and the small magnitude of k_1 (vide supra)), this expression further simplifies to eq 5. Substituting the rate constants that we obtained into eq 5 yields a composite of these rate constants ($k_{\text{obs}} = k_1 k_2 [Ru]_0 / (k_{-1} [4]_0)$). This produces $k_{\text{obs}} = 9.89 \times 10^{-5} \text{ s}^{-1}$, which can be compared with $k_{\text{obs}} = 8.81 \times 10^{-5} \text{ s}^{-1}$ obtained from a curve fit of [4] versus time (Figure 8), suggesting that the highly simplified eq 5 represents a useful model for this reaction.^{37,38}

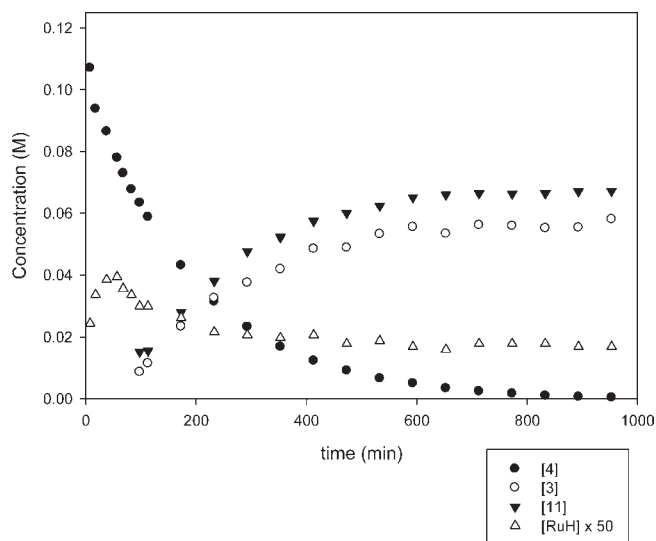
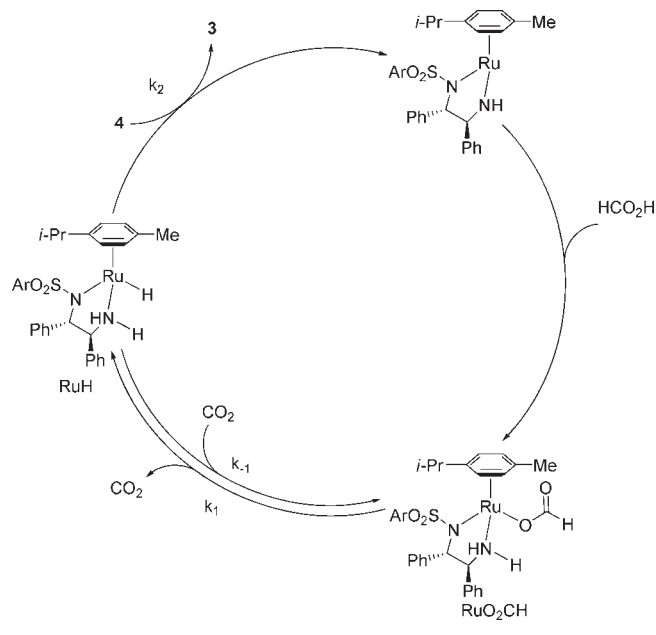


Figure 8. Concentrations of 4, 3, 11, and Ru-hydride ($[RuH] \times 50$) vs time.

Scheme 8. Catalytic Cycle for Transfer Hydrogenation Using Formic Acid



Equation 5 clearly explains the dichotomous behavior of this kinetic system, wherein overall rates are unaffected by changing $[4]_0$, but a given reaction exhibits a first-order decay of 4. When $[4]_0$ was changed from 0.125 to 0.0625 M to 0.03125 M (Table 2), both $[4]_0$ and $[4]$ changed proportionally, resulting in no net effect on reaction rate ($-d[4]/dt$), and corresponding to a 2- and 4-fold increase in $k_{\text{obs}} = (-d[4]/dt)/[4]$. In contrast, throughout the course of a reaction, the denominator in eq 5 (or eq 3) remains constant, while $[4]$ in the numerator follows a first-order decay, leading to the observed first-order kinetics. A physical interpretation of this kinetic data is that even though the reaction of Ru-hydride with imine 4 is fast compared to the conversion of Ru-formate to Ru-hydride, the generation of CO₂ as a byproduct inhibits the reaction as it progresses, pushing

the equilibrium away from Ru–hydride, and yielding a decrease in rate and an apparent first-order dependence on **4**.

$$-\frac{d[\mathbf{4}]}{dt} = k_2[\text{RuH}][\mathbf{4}] \quad (1)$$

$$\begin{aligned} \frac{-d[\text{RuH}]}{dt} &= 0 \\ &= k_1[\text{RuO}_2\text{CH}] - k_{-1}[\text{RuH}][\text{CO}_2] - k_2[\text{RuH}][\mathbf{4}] \end{aligned} \quad (2)$$

$$\frac{-d[\mathbf{4}]}{dt} = \frac{k_1 k_2 [\text{Ru}]_0 [\mathbf{4}]}{k_{-1} [\text{CO}_2] + k_2 [\mathbf{4}] + k_1} \quad (3)$$

$$\frac{-d[\mathbf{4}]}{dt} \approx \frac{k_1 k_2 [\text{Ru}]_0 [\mathbf{4}]}{k_{-1} [\mathbf{4}]_0 + (k_2 - k_{-1}) [\mathbf{4}] + k_1} \quad (4)$$

$$\frac{-d[\mathbf{4}]}{dt} \approx \frac{k_1 k_2 [\text{Ru}]_0 [\mathbf{4}]}{k_{-1} [\mathbf{4}]_0} \quad (5)$$

REMOVAL OF CO₂ FROM REACTION MIXTURE

The above mechanistic investigations suggested that purging of CO₂ during an asymmetric reductive amination in acetonitrile/toluene on larger scale would accelerate the reaction rate. Side-by-side experiments were conducted in Multimax vessels equipped with ReactIR probes to directly compare the effects of nitrogen purging with no purging. Even though an IR probe could not effectively distinguish between compounds **4** and **3**, it clearly showed a strong band for CO₂ at 2339 cm⁻¹. The vessel undergoing the nitrogen sweep showed <5% of the [CO₂] found in the sealed control vessel. This decrease in [CO₂] was accompanied by a ~60% increase in the reaction rate, allowing the loading of catalyst **10** to be decreased to 2 mol %. Additionally, isolated yields were always greater in purged reactions (by up to 20%) since there was no appreciable formation of carbamates and subsequent loss into basic aqueous layers during work-up.

To investigate whether rate acceleration by CO₂ removal is a general phenomenon, the transfer hydrogenation of acetophenone with this same catalyst system was examined. The effects of purging should be even more pronounced in a ketone reduction reaction, since there are no amines produced to absorb some of the CO₂. An alternative to CO₂ purging could be accomplished by trapping with a secondary amine, similar to the carbamate formation in the reductive amination step. Thus, the effects of purging and trapping of CO₂ on the transfer hydrogenation rates of acetophenone (Scheme 9) were examined when using 10 mol % Ru under conditions that were otherwise identical to those used for the reductive amination.

Addition of piperidine and, particularly, pyrrolidine proved effective at trapping CO₂, resulting in rate enhancements of ~2.5- and 3.7-fold, respectively, versus reactions using triethylamine (Figure 9).^{39,40} Purging CO₂ proved even more effective, resulting in a remarkable 9.5-fold increase in rate over a sealed reaction using triethylamine. In all cases, the transfer hydrogenation reaction of acetophenone gave 98.3–98.9% ee.

Scheme 9. Transfer Hydrogenation of Acetophenone

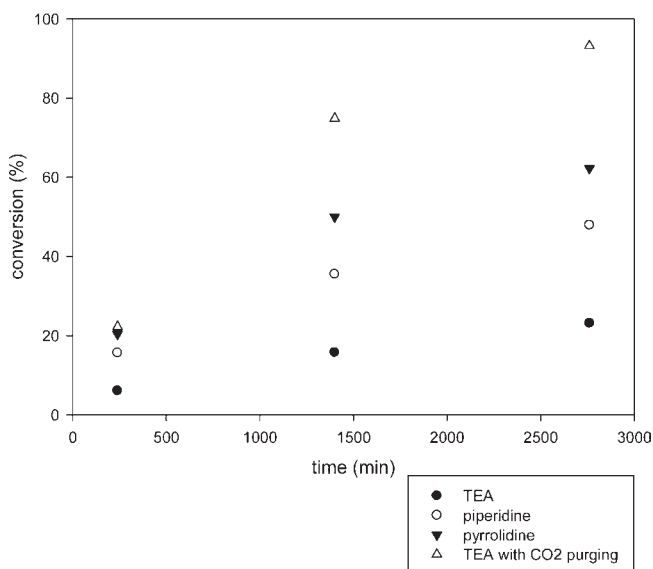
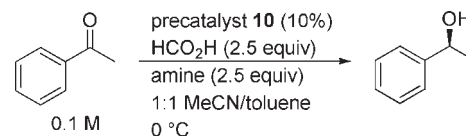


Figure 9. Conversion of acetophenone vs time as a function of amine.

SUMMARY

The first asymmetric reductive amination of a dialkyl ketone with an alkylamine was developed using a new variant of Noyori's (*S,S*)-RuCl(*p*-cymene)(ArSO₂DPEN) catalyst. This process proceeds with high yield (>97%) and high enantioselectivity (>94%) to form a diazepane ring in the key step of the synthesis of a novel dual Orexin inhibitor and has been run on >100 kg scale. Despite the requirements of low temperature, high pH, high dilution, and bulky catalyst needed to provide high yield and ee, a reduction of the catalyst loading to 2 mol % proved feasible. In the course of this work, the profound impact of CO₂ on the equilibrium between Ru–hydride and Ru–formate catalyst forms and the corresponding negative effects that CO₂ had on reaction rate were studied. The potential of formation of carbamates of the product with CO₂ was noted as this can reduce the overall isolated yield. Incorporating a purge of CO₂ into the process led to an increase in the rate of reaction and allowed for product isolation with a nearly quantitative yield. Finally, significant rate increases in the transfer hydrogenation of acetophenone (either via purging of the reaction mixture, or trapping with secondary amines) were realized, suggesting that this may be a generally useful technique.

EXPERIMENTAL SECTION

Asymmetric Reductive Amination in CH₂Cl₂ and Upgrade via HCl Salt (R**)-**3**.** *Catalyst Preparation.* Dichloromethane (68 mL), ligand (*S,S*)-**9** (300 mg), [RuCl₂(*p*-cymene)]₂ (191 mg), and triethylamine (1.29 g) were combined to give an orange slurry which was

heated to 40 °C for 3 h leading to an orange/red solution which was cooled to room temperature.

In a second vessel, dichloromethane (200 mL) was charged and degassed via nitrogen pressure purges. Bis(MSA) salt 2-MSA (10 g) and anhydrous potassium carbonate powder (325 mesh; 11.6 g) were added followed by water (1.16 mL). The vessel contents were then cooled to -10 to -5 °C. Triethylamine (5.34 g) was charged to the mixture followed by the preformed catalyst solution. The solution was degassed by nitrogen purge and then formic acid (1.28 g) was added. This was followed by a second formic acid charge of 2.60 g after 30 min. The reaction temperature was maintained at -10 to -5 °C and the mixture aged for 16 h.

The reaction was quenched by addition of NaOH solution (123 g, 1.0 M, aq), the layers were allowed to separate, and the lower organic layer was collected. The organic layer was then concentrated, then toluene (68 mL) and DMAc (34 mL) were added followed by anhydrous HCl (2.26 g). The salt was cooled to 0 °C over 3 h, and the solids were isolated by filtration. The solids were dried at 40 °C to afford 5.48 g of amine HCl salt (*R*)-3-HCl, 87% yield, >99.9% purity and 99.7% ee. **3** (free base): ¹H NMR (500 MHz, CD₂Cl₂) δ 7.22 (d, *J* = 2.1 Hz, 1H), 7.146 (d, *J* = 8.2 Hz, 1H), 6.93 (dd, *J* = 8.4, 2.6 Hz, 1H), 3.90 (ddd, *J* = 14.5, 6.1, 4.1 Hz, 1H), 3.80 (dt, *J* = 13.7, 3.3 Hz, 1H), 3.68–3.56 (m, 2H), 3.20 (dt, *J* = 14.2, 3.5 Hz, 1H), 2.92 (ddd, *J* = 14.2 Hz, 11.0, 3.5 Hz, 1H), 2.77 (dq, *J* = 9.9, 6.4, 3.3 Hz, 1H), 1.94 (ddt, *J* = 14.3, 6.0, 3.2 Hz, 1H), 1.59–1.46 (m, 2H), 1.10 (d, *J* = 6.4 Hz, 3H); ¹³C NMR (126 MHz, CD₂Cl₂) δ 164.10, 148.30, 146.06, 129.39, 119.97, 116.09, 109.55, 55.76, 51.68, 48.13, 46.59, 38.40, 23.58; IR (cm⁻¹): 1249, 1571, 1639; LCMS: [M + H]⁺ calcd for C₁₃H₁₆ClN₃O + H⁺, 266.1; found 265.9, 267.9 (30%).

■ ASSOCIATED CONTENT

S Supporting Information. Experimental procedures, characterization data, and copies of NMR spectra. This material is available free of charge via the Internet at <http://pubs.acs.org>.

■ AUTHOR INFORMATION

Corresponding Author

neil_strotman@merck.com

■ ACKNOWLEDGMENT

We would like to thank Mike Ashwood, Brian Bishop, John Edwards, David Lieberman, and Faye Sheen (Department of Process Research, Hoddessdon, U.K.), and Paul Fernandez, Tony Moses, Marguerite Mohan, Doris Glykys and Robert Scogna (Department of Chemical Process Development and Commercialization, Rahway, NJ) for experimental input.

■ REFERENCES

- (1) Cox, C. D.; *J. Med. Chem.* **2010**, *53*, 5320–5332.
- (2) Baxter, C. A.; Cleator, D.; Brands, K. M. J.; Edwards, J. S.; Reamer, R. A.; Sheen, F. J.; Stewart, G. W.; Strotman, N. A.; Wallace, D. J. *Org. Process. Res. Dev.* **2011**, *15*, 367–375.
- (3) The one exception to the ubiquitous low selectivity for reduction of unbranched dialkylimines was from the work of MacMillan et al. which demonstrated asymmetric reductive amination of 2-butanone with 4-methoxyaniline using a chiral phosphoric acid derivative. Storer, R. I.; Carrera, D. E.; Ni, Y.; MacMillan, D. W. C. *J. Am. Chem. Soc.* **2006**, *128*, 84–86.
- (4) It has been shown that transfer hydrogenation proceeds >1000 times faster for imines than for structurally similar ketones: Uematsu, N.;

Fujii, A.; Hashiguchi, S.; Ikariya, T.; Noyori, R. *J. Am. Chem. Soc.* **1996**, *118*, 4916–4917.

(5) For examples of asymmetric imine hydrogenation or reductive amination using H₂, see: (a) Blaser, H.-U.; Buser, H. P.; Jalett, H. P.; Pugin, B.; Spindler, F. *Synlett* **1999**, 867. (b) Kadyrov, R.; Reirmeier, T. H. *Angew. Chem., Int. Ed.* **2003**, *42*, 5472–5474. (c) Kadyrov, R.; Riermeier, T. H.; Dingerdissen, W.; Tararov, V.; Börner, A. *J. Org. Chem.* **2003**, *68*, 4067–4070. (d) Chi, Y.; Zhou, Y.-G.; Zhang, X. *J. Org. Chem.* **2003**, 4120–4122. (e) Börner, A. *Synlett* **2005**, 203–211.

(6) Noyori's preformed Ru catalysts of the form RuCl₂(diamine)-(bis-phosphine) exhibited low yields (<30%) and ee's (<20%).

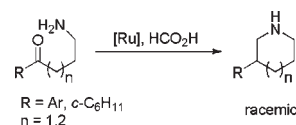
(7) Yamada, K.; Takeda, M.; Wakuma, I. *Tetrahedron Lett.* **1981**, 3869.

(8) Attempts to carry out transfer hydrogenation using [RuCl₂(*p*-cymene)]₂ and amino alcohol ligands in IPA with KOH resulted in none of the desired reductive amination product and only some ketone reduction.

(9) RuCl(*p*-cymene)(Ts-DPEN) was developed for transfer hydrogenation of ketones using IPA as the hydrogen donor. It was later shown that IPA could be replaced by formic acid to give an irreversible reaction through generation of CO₂. (a) Hashiguchi, S.; Fujii, A.; Takehara, J.; Ikariya, T.; Noyori, R. *J. Am. Chem. Soc.* **1995**, *117*, 7562–7563. (b) Fujii, A.; Hashiguchi, S.; Uematsu, N.; Ikariya, T.; Noyori, R. *J. Am. Chem. Soc.* **1996**, *118*, 2521–2522.

(10) (a) Noyori, R.; Hashiguchi, S. *Acc. Chem. Res.* **1997**, *30*, 97–102. (b) Palmer, M. J.; Wills, M. *Tetrahedron Asym.* **1999**, *10*, 2045–2061.

(11) Wills found that RuCl(*p*-cymene)(TsDPEN) gave nearly racemic products in similar intramolecular reductive amination reactions to give 6 or 7-membered rings, and gave very low yields of 7-membered ring products. Williams, G. D.; Pike, R. A.; Wade, C. E.; Wills, M. *Org. Lett.* **2003**, *5*, 4227–4230.



(12) Wills has shown that certain monocyclic imines can be hydrogenated with up to 60% ee using N-alkylated variants of **5**. Martins, J. E. D.; Redonde, M. A. C.; Wills, M. *Tetrahedron: Asymmetry* **2010**, *21*, 2258–2264.

(13) Mohar, B.; Valleix, A.; Desmurs, J.-R.; Felemez, M.; Wagner, A.; Mioskowski, C. *Chem. Commun.* **2001**, 2572–2573.

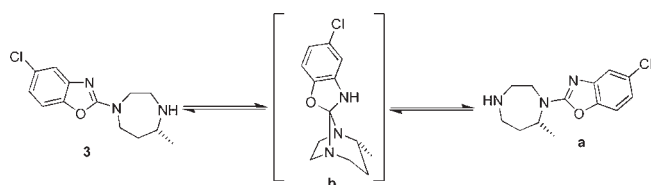
(14) We initially attempted to preform imine **4** by treatment with sodium formate and MgSO₄ to deprotonate 2-MSA and remove water, respectively.

(15) Xiao and co-workers reported highly enantioselective imine hydrogenation and reductive amination of acetophenone derivatives using a Cp*IrX complex with **9** using a chiral phosphoric acid additive. Additionally, they reported reductive amination of unbranched dialkyl ketones using a Cp*IrX Me₃C₆SO₂-DPEN complex and a chiral phosphoric acid that proceeded with high ee. This system was not applicable to aliphatic amines and the addition of chiral phosphoric acids to our process led to no improvement in rate or ee. (a) Li, C.; Wang, C.; Villa-Marcos, B.; Xiao, J. *J. Am. Chem. Soc.* **2008**, *130*, 14450–14451. (b) Li, C.; Villa-Marcos, B.; Xiao, J. *J. Am. Chem. Soc.* **2009**, *131*, 6967–6969.

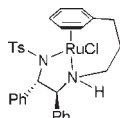
(16) In experiments with only Et₃N as base, we found that when mesylate ion is present in solution as ammonium salts, the reaction proceeds quickly but with lower enantioselectivity. When mesylate is removed from solution by precipitation as the potassium or cesium salt (as determined by ¹H NMR), the reaction is slower, but proceeds with high ee.

(17) During formation and manipulation of the DBT (dibenzoyltartrate) salt of **3**, up to 20% of an impurity had formed that was determined to be isomer **a**, which could be formed through bicyclic 5.6-ring species **b**. While weak acids like pivalic acid readily catalyzed this

process, stronger acids led to minimal isomerization (see Supporting Information for effect of acid pK_a ; Table S1).



(18) A tethered variant of **5**, [(*s,s*)-teth-TsDPEN-RuCl], originally developed by Wills, provided low conversion and 63% ee under otherwise identical conditions. Hayes, A. M.; Morris, D. J.; Clarkson, G. J.; Wills, M. *J. Am. Chem. Soc.* **2005**, *127*, 7318–7319.



(19) $[\text{HCO}_2\text{H}]_0 = [\text{TEA}]_0 = 0.3125 \text{ M}$ in all reactions.

(20) Since the product (**3**) of asymmetric reductive amination generally precipitated late in the reaction as the formate salt, kinetics were generally studied by setting up a series of identical reactions for one run and quenching them at various times. This was the only way that we could accurately determine the ee of the product as a function of conversion/time.

(21) Rates determined by fitting $[\mathbf{4}] = [\mathbf{4}]_0 e^{-kt}$.

(22) Cheung, F. K.; Lin, C.; Minissi, F.; Criville, A. L.; Graham, M. A.; Fox, D. J.; Wills, M. *Org. Lett.* **2007**, *9*, 4659–4662.

(23) Casey and Johnson provided evidence for the concerted nature of the proton and hydride transfer to ketones through deuterium kinetic isotope effect studies. Casey, C. P.; Johnson, J. B. *J. Org. Chem.* **2003**, *68*, 1998–2001.

(24) It was shown by Bäckvall that the presence of acid was critical for activity toward imine hydrogenation with this catalyst system, suggesting that an iminium species, rather than an imine is actually being reduced Åberg, J. B.; Samec, J. S. M.; Bäckvall, J.-E. *Chem. Commun.* **2006**, 2771–2773.

(25) Both Wills and Pihko have suggested an ionic transition state involving attack of the Ru–hydride moiety on a protonated imine or iminium ion. (a) Martins, J. E. D.; Clarkson, C. J.; Wills, M. *Org. Lett.* **2009**, *11*, 847–850. (b) Evanno, L.; Ormala, J.; Pihko, P. M. *Chem.—Eur. J.* **2009**, *15*, 12963–12967.

(26) Koike, T.; Ikariya, T. *Adv. Synth. Catal.* **2004**, *346*, 37–41.

(27) For examples of equilibria between metal hydrides and CO_2 with formates see the following, and references therein: Creutz, C.; Chou, M. H. *J. Am. Chem. Soc.* **2009**, *131*, 2794–2795.

(28) Haack, K.-J.; Hashiguchi, S.; Fujii, A.; Ikariya, T.; Noyori, R. *Angew. Chem., Int. Ed. Engl.* **1997**, *36*, 285–288.

(29) Cheung, F. K.; Clarke, A. J.; Clarkson, G. J.; Fox, D. J.; Graham, M. A.; Lin, C.; Crivillé, A. L.; Wills, M. *Dalton Trans.* **2010**, *39*, 1395–1402.

(30) Since the Ru–hydride is a saturated 18-electron species, its reaction with CO_2 most likely does not involve CO_2 coordination to Ru since this would require either partial ligand dissociation or an η^6 to η^4 ring slip, both high energy processes. A more likely explanation is that CO_2 hydrogen bonds to the NH_2 of the catalyst, adds hydride to generate formate, and since formate is an insufficiently strong base to deprotonate the Ru-coordinated NH_2 moiety (unlike alkoxide, from ketone reduction), the formate then coordinates to Ru.

(31) See Supporting Information (Figure S1).

(32) No precipitation of **3** as the formate salt was observed in an NMR tube.

(33) Rate determined by fitting $[\mathbf{4}] = [\mathbf{4}]_0 e^{-kt}$ (See Supporting Information, Figure S2 for curve fit).

(34) See Supporting Information (Figure S3) for a plot of k_2 vs time, where $k_2 = (-d[\mathbf{4}]/dt)/([\text{RuH}][\mathbf{4}]) = k_{\text{obs}}/[\text{RuH}]$. This value for k_2

was estimated using data between 200 and 600 min, since in this region the value of $[\text{Ru–hydride}]$ was not changing drastically, and there was a relatively small error in the rate measurement compared to late in the reaction.

(35) The equilibrium constant was determined by measuring $[\text{Ru–hydride}]$ and $[\text{Ru–formate}]$ by ^1H NMR and $[\text{CO}_2]$ by ^{13}C NMR (relative to the $\text{CD}_3\text{CN}/\text{toluene-}d_8$ solvent mixture) in a sealed NMR tube at 0°C using the following relationship: $K_{\text{eq}} = k_1/k_{-1} = [\text{Ru–hydride}][\text{CO}_2]/[\text{Ru–formate}] = 0.014 \text{ M}$.

(36) $[\text{CO}_2] = [\mathbf{4}]_0 - [\mathbf{4}] - [\mathbf{11}] - [\text{CO}_2]_{\text{g}} = [\mathbf{3}]_t - [\text{CO}_2]_{\text{g}}$, where $[\text{CO}_2]_{\text{g}}$ = moles of CO_2 in gas phase divided by volume of reaction mixture. This does not take into account the minor impact of the Ru–hydride/Ru–formate equilibrium on $[\text{CO}_2]$.

(37) See Supporting Information (Figure S4) for overlaid plots of experimental and calculated $[\mathbf{4}]$ vs time ($[\mathbf{4}]$ calculated using $k_{\text{obs}} = k_1 k_2 [\text{Ru}]_0 / (k_{-1} [\mathbf{4}]_0)$).

(38) A major source of error in this rate law is the use of the steady-state approximation for $[\text{Ru–hydride}]$. It is clear from Figure 8 that $[\text{Ru–hydride}]$ changes considerably over the course of the reaction, as the initially formed Ru–formate is converted to Ru–hydride to establish equilibrium and then after reaching a maximum, Ru–hydride begins to decrease as CO_2 is produced and the equilibrium is shifted toward Ru–formate.

(39) Relative rates assuming first-order kinetics in [acetophenone].

(40) Amine **3** appears to be a highly effective trapping agent for CO_2 . When 1 equiv of acetophenone was added to the standard asymmetric reductive amination reaction of **4**, the acetophenone was hydrogenated 4 times faster than acetophenone in a similar reaction without **4** (29% vs 8% conversion). The high nucleophilicity of this diazepane ring in **3** is consistent with the relative order of nucleophilicity of secondary amines: piperidine < pyrrolidine < piperazine < homopiperidine. Brotzel, F.; Chu, Y. C.; Mayr, H. *J. Org. Chem.* **2007**, *72*, 3679–3688.